Part VI

Summary of QCD tests and α_s measurements

VI.1 The different observables

We have discussed in the previous two parts of this book, deep inelastic scatterings in hadron colliders and different hard processes in e^+e^- annihilations. These hard processes have been used for testing the underlying ideas of perturbative QCD at short distances. Among others, one has studied and measured:

- Scaling violations in different parton model sum rules.
- Structure functions.
- Spin content of the proton.
- Fragmentation functions.
- Spin of the photon.
- One hadron inclusive production.
- Jets.
- Total inclusive e^+e^- cross-sections.
- Hadronic τ and Z^0 decays.

In all these hard processes, most of the perturbative QCD predictions based on the $SU(3)_c$ colour group and on asymptotic freedom properties have been confirmed by the data.

VI.2 Different tests of QCD

The main outcomes of these analysis in the previous parts of the book are given in the following sections.

VI.2.1 Deep inelastic scatterings

- A measurement of the scaling violations to parton model predictions in deep inelastic processes using different moments of the structure functions as predicted by QCD. In the unpolarized case, one has used these processes to extract the value of the QCD running coupling. In the polarized case, one has been able to emphasize the important universal rôle of the QCD anomaly for explaining the relative suppression of the first moment of the structure function compared to the OZI prediction (so-called proton spin) and a proposal for testing its effect from the measurement of the photon spin in γ-γ scattering processes, and of some semi-inclusive processes.

https://doi.org/10.1017/9781009290296.035 Published online by Cambridge University Press

- An extension of the test of the validity of perturbation theory in the low-x region leading to a modification of the Altarelli–Parisi evolution equations.

VI.2.2 QCD jets

- A confirmation of the vector nature of the gluon rather than its scalar nature from the measurement of the moment distributions in three-jet events.
- A measurement of the ratio of the colour group factor C_A/C_F from the scaling violation rates in inclusive hadron distributions and charged hadron multiplicites from gluon and quark jets, which leads to

$$\frac{C_A}{C_F} = 2.24 \pm 0.11 \,, \tag{VI.1}$$

in agreement with the QCD expectation:

$$\frac{C_A}{C_F} = 9/4 = 2.25 \,. \tag{VI.2}$$

This fact confirms the $SU(3)_c$ colour group structure of QCD for describing the strong interactions, and the appearance of the different vertices involving gluon interactions. It also rules out some other group candidates (Abelian, semi-simple Lie group . . .).
- An extraction of the QCD running coupling α_s.

Inclusive e^+e^-, $Z \to$ hadrons and $\tau \to \nu_\tau$ hadrons processes

- Most precise extractions of the QCD running coupling α_s using the high statistics LEP measurements of the $Z \to$ hadrons and $\tau \to \nu_\tau +$ hadrons decays and the best QCD approximation available today (NNLO and resummation of the asymptotic terms of the QCD series). Unlike the previous deep inelastic and jet processes, one does not need to introduce structure and/or fragmentation functions which can limit the accuracy of the predictions.

VI.3 Summary of the α_s determinations

- In the massless quark limits which are a good approximation for the light quarks, QCD is a one-parameter theory gouverned by its running coupling $\alpha_s(Q^2)$ evaluated at a scale Q, such that all hard strong interaction processes, where one can apply perturbative QCD, should be described in terms of this single input parameters.
- A determination of the values of the running QCD coupling $\alpha_s(Q^2)$ at different energies from various processes as summarized in the table and figures from [139]. In this comparison, the coupling should be defined in the same way everywhere. The $\overline{MS}$ scheme has been adopted as the most convenient renormalization scheme for defining this coupling.

One can see that the running of the coupling shown in Fig. VI.1 from 1 to 100 GeV and at LEP2 energies in Fig. VI.2 satisfies the $1/\log$ behaviour predicted by QCD. The slope of the curve interpreted in terms of the first coefficient of the β function lead to an alternative measurement of

https://doi.org/10.1017/9781009290296.035 Published online by Cambridge University Press

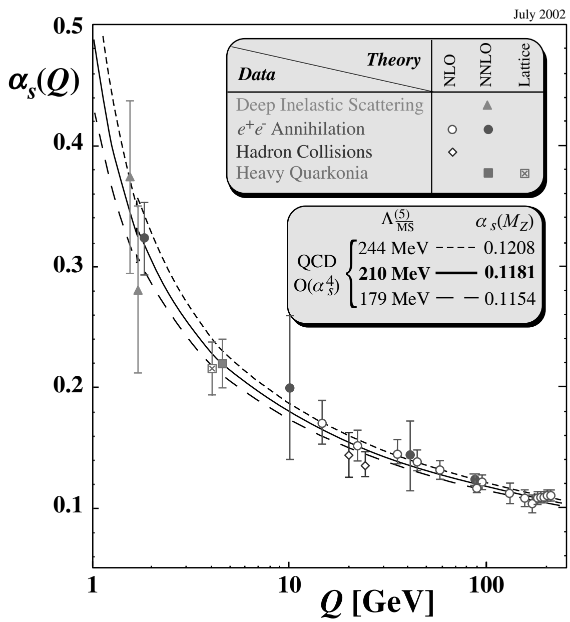

Fig. VI.1. Summary of the different α_s determinations at different energies from [139].

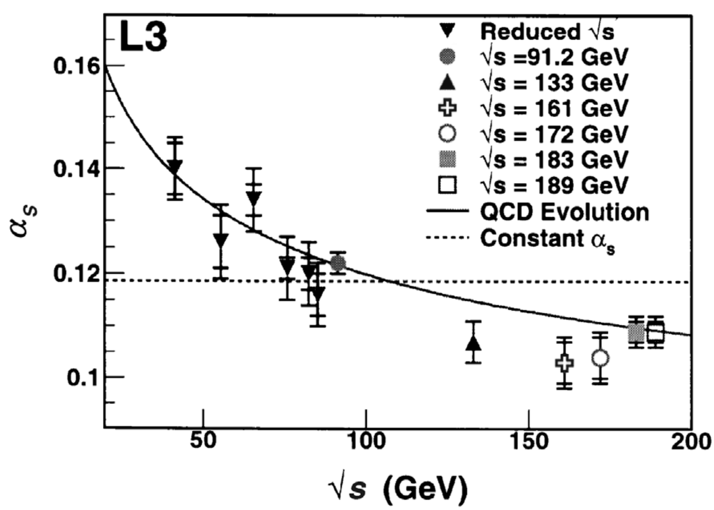

Fig. VI.2. α_s determinations from hadronic event shapes at LEP2 energies.

the number of colours:

$$N_c = 3.03 \pm 0.12\,, \tag{VI.3}$$

which is an internal consistency check of the results between data and QCD ($N_c = 3$ in QCD!).

- Evaluated at the common scale $Q = M_{Z^0}$, the different experiments lead to consistent values of α_s as shown in Fig. VI.3, with the average value from the six most significant NNLO determinations

https://doi.org/10.1017/9781009290296.035 Published online by Cambridge University Press

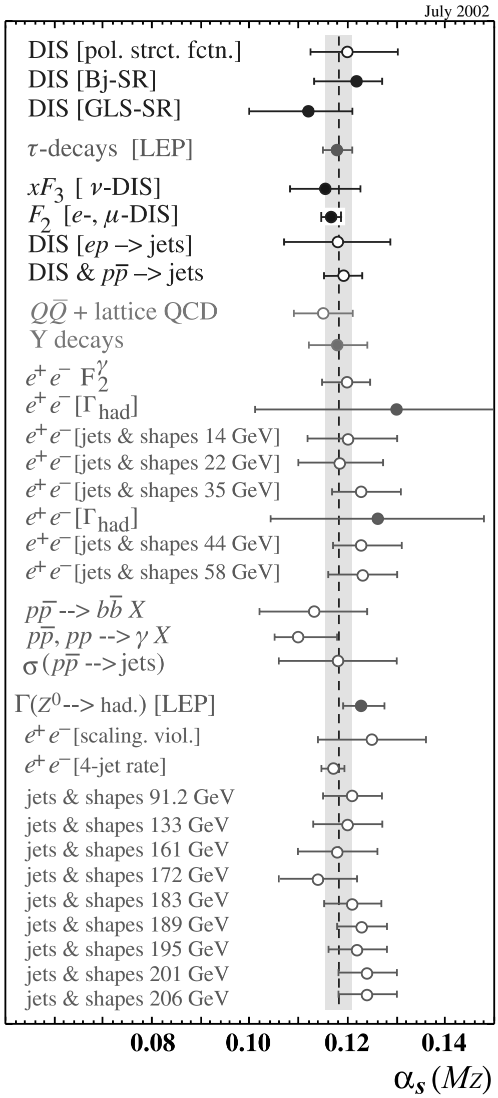

Fig. VI.3. Summary of the different α_s determinations at the common scale M_{Z^0} from [139].

(total error less or equal than 0.008) [139]:[1]

$$\alpha_s(M_{Z^0}) = 0.1181 \pm 0.0027\,. \tag{VI.4}$$

As a result, the corresponding value of the QCD scale for five flavours is:

$$\Lambda_5 = \left(210^{+34}_{-31}\right)\,\text{MeV}\,. \tag{VI.5}$$

[1] The one coming from PDG 2000 [16] is slightly more precise than the average of different determinations from Table VI.1. This is mainly due to the inclusion of the result from [250], where the error of 0.001 has been taken literally.

https://doi.org/10.1017/9781009290296.035 Published online by Cambridge University Press

Table VI.1. *World summary of measurements of α_s (status of July 2002) from [139]: DIS = deep inelastic scattering; GLS-SR = Gross–Llewellyn-Smith sum rule; Bj-SR = Bjorken sum rule; (N)NLO = (next-to-) next-to-leading order perturbation theory; LGT = lattice gauge theory; resum. = resummed NLO). Some entries are still preliminary.*

Process	Q [GeV]	$\alpha_s(Q)$	$\alpha_s(M_Z)$	$\Delta\alpha_s(M_Z)$ exp.	$\Delta\alpha_s(M_Z)$ theor.	Theory
DIS [pol. strct. fctn.]	0.7–8		$0.120\,^{+0.010}_{-0.008}$	$^{+0.004}_{-0.005}$	$^{+0.009}_{-0.006}$	NLO
DIS [Bj-SR]	1.58	$0.375\,^{+0.062}_{-0.081}$	$0.121\,^{+0.005}_{-0.009}$	–	–	NNLO
DIS [GLS-SR]	1.73	$0.280\,^{+0.070}_{-0.068}$	$0.112\,^{+0.009}_{-0.012}$	$^{+0.008}_{-0.010}$	0.005	NNLO
τ-decays	1.78	0.323 ± 0.030	0.1181 ± 0.0031	0.0007	0.0030	NNLO
DIS [ν; xF_3]	2.8–11		0.1153 ± 0.0073	0.0040	0.0061	NNLO
DIS [e/μ; F_2]	1.9–15.2		0.1166 ± 0.0022	0.0009	0.0020	NNLO
DIS [e-p $\to$ jets]	6–100		0.118 ± 0.011	0.002	0.011	NLO
DIS & p$\bar{\text{p}}$ $\to$jets	1–400		0.119 ± 0.004	0.002	0.003	NLO
Q$\bar{\text{Q}}$ states	4.1	0.216 ± 0.022	0.115 ± 0.006	0.000	0.006	LGT
Υ decays	4.75	0.217 ± 0.021	0.118 ± 0.006	–	–	NNLO
e^+e^- [F_2^γ]	1.4–28		$0.1198\,^{+0.0044}_{-0.0054}$	0.0028	$^{+0.0034}_{-0.0046}$	NLO
e^+e^- [σ_{had}]	10.52	0.20 ± 0.06	$0.130\,^{+0.021}_{-0.029}$	$^{+0.021}_{-0.029}$	0.002	NNLO
e^+e^- [jets & shapes]	14.0	$0.170\,^{+0.021}_{-0.017}$	$0.120\,^{+0.010}_{-0.008}$	0.002	$^{+0.009}_{-0.008}$	resum
e^+e^- [jets & shapes]	22.0	$0.151\,^{+0.015}_{-0.013}$	$0.118\,^{+0.009}_{-0.008}$	0.003	$^{+0.009}_{-0.007}$	resum
e^+e^- [jets & shapes]	35.0	$0.145\,^{+0.012}_{-0.007}$	$0.123\,^{+0.008}_{-0.006}$	0.002	$^{+0.008}_{-0.005}$	resum
e^+e^- [σ_{had}]	42.4	0.144 ± 0.029	0.126 ± 0.022	0.022	0.002	NNLO
e^+e^- [jets & shapes]	44.0	$0.139\,^{+0.011}_{-0.008}$	$0.123\,^{+0.008}_{-0.006}$	0.003	$^{+0.007}_{-0.005}$	resum
e^+e^- [jets & shapes]	58.0	0.132 ± 0.008	0.123 ± 0.007	0.003	0.007	resum
p$\bar{\text{p}}$ $\to$ b$\bar{\text{b}}$X	20.0	$0.145\,^{+0.018}_{-0.019}$	0.113 ± 0.011	$^{+0.007}_{-0.006}$	$^{+0.008}_{-0.009}$	NLO
p$\bar{\text{p}}$, pp $\to \gamma$X	24.3	$0.135\,^{+0.012}_{-0.008}$	$0.110\,^{+0.008}_{-0.005}$	0.004	$^{+0.007}_{-0.003}$	NLO
σ(p$\bar{\text{p}}$ $\to$ jets)	40–250		0.118 ± 0.012	$^{+0.008}_{-0.010}$	$^{+0.009}_{-0.008}$	NLO
e^+e^- [$\Gamma(Z^0 \to$ had.)]	91.2	$0.1227^{+0.0048}_{-0.0038}$	$0.1227^{+0.0048}_{-0.0038}$	0.0038	$^{+0.0029}_{-0.0005}$	NNLO
e^+e^- scal. viol.	14–91.2		0.125 ± 0.011	$^{+0.006}_{-0.007}$	0.009	NLO
e^+e^- four-jet rate	91.2	0.1170 ± 0.0026	0.1170 ± 0.0026	0.0001	0.0026	NLO
e^+e^- [jets & shapes]	91.2	0.121 ± 0.006	0.121 ± 0.006	0.001	0.006	resum
e^+e^- [jets & shapes]	133	0.113 ± 0.008	0.120 ± 0.007	0.003	0.006	resum
e^+e^- [jets & shapes]	161	0.109 ± 0.007	0.118 ± 0.008	0.005	0.006	resum
e^+e^- [jets & shapes]	172	0.104 ± 0.007	0.114 ± 0.008	0.005	0.006	resum
e^+e^- [jets & shapes]	183	0.109 ± 0.005	0.121 ± 0.006	0.002	0.005	resum
e^+e^- [jets & shapes]	189	0.109 ± 0.004	0.121 ± 0.005	0.001	0.005	resum
e^+e^- [jets & shapes]	195	0.109 ± 0.005	0.122 ± 0.006	0.001	0.006	resum
e^+e^- [jets & shapes]	201	0.110 ± 0.005	0.124 ± 0.006	0.002	0.006	resum
e^+e^- [jets & shapes]	206	0.110 ± 0.005	0.124 ± 0.006	0.001	0.006	resum

- However, one should have in mind that the different values of α_s for each process are not obtained within the same QCD approximations. In some processes, they are known very precisely to NNLO, while in some others they are poorly known to NLO. In addition, the theoretical uncertainties are also affected by the asymptotic behaviour of the perturbative series in powers of α_s, and by small non-perturbative effects which should be present in different processes. We shall come back to this point in subsequent chapters.